Supporting Information

Van der Waals heterojunction devices based on organohalide perovskites and two-dimensional materials

Hung-Chieh Cheng,[†] Gongming Wang,[‡] Dehui Li,[‡] Qiyuan He,[‡] Anxiang Yin,[‡] Yuan Liu,[†] Hao Wu,[†] Mengning Ding,[†] Yu Huang,[†,§] and Xiangfeng Duan[‡,§]*

[†]Department of Materials Science and Engineering, [‡]Department of Chemistry and Biochemistry, University of California, Los Angeles, CA 90095, USA

[§]California Nanosystems Institute, University of California, Los Angeles, CA 90095, USA

Outline

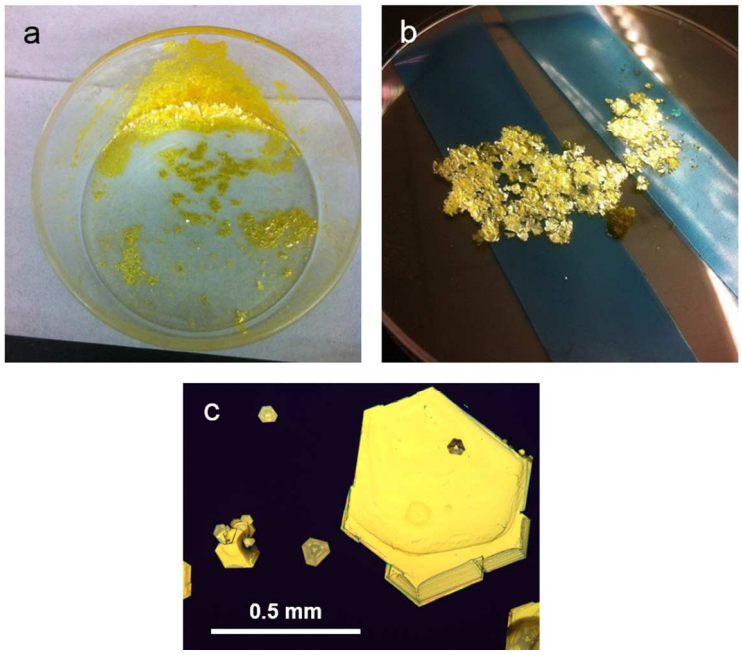

Figure S1. Dried PbI_2 crystal for mechanical exfoliation. (a) Precipitated PbI_2 crystal after drying the supersaturated solution in oven. (b) The crystal can be easily peeled off from the glass dish by commercial adhesive tape. (c) The zoom-in image of a precipitated PbI_2 crystal.

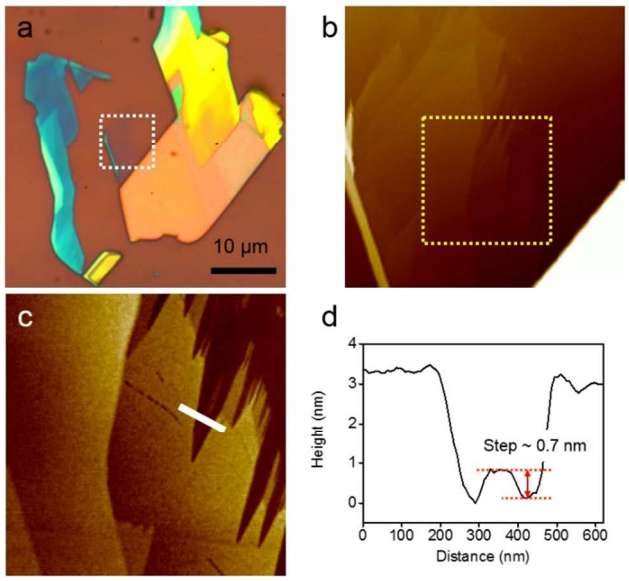

Figure S2. Optical and AFM images of exfoliated few layer and monolayer PbI_2. (a) Optical image of PbI_2 exfoliated by micromechanical cleavage on silicon substrate with SiO_2 (290 nm). (b) AFM image was obtained by scanning the area marked by the white dashed square in **a**. The topography distribution shows layered nature of exfoliated PbI_2. (c) A further zoom-in scanning results from the yellow dashed square in (b). (d) The height profile from the cross-section of the thinnest flake we can find (indicated by white line shown in (c)). The height is ~ 0.7 nm which is quite consistent with the reported monolayer PbI_2 thickness.[1]

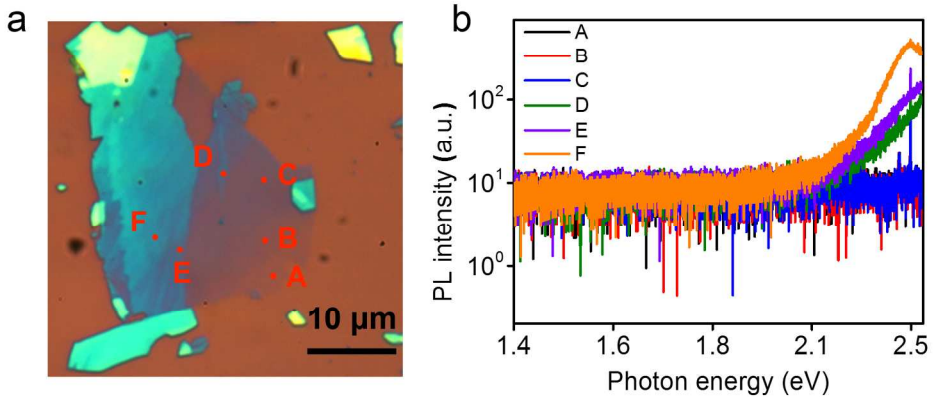

Figure S3. Thickness dependent photoluminescence (PL) spectra of an exfoliated ultrathin PbI_2 flakes. (a) Optical image of an exfoliated PbI_2 flake. The red dots represent the laser spot of PL measurement. (b) PL spectra taken at corresponding spots shown in (a). The thickest part shows a prominent PL peak. As the thickness decrease, the PL peaks blue shift[2] and dim out of detection limit of our measurement set up.

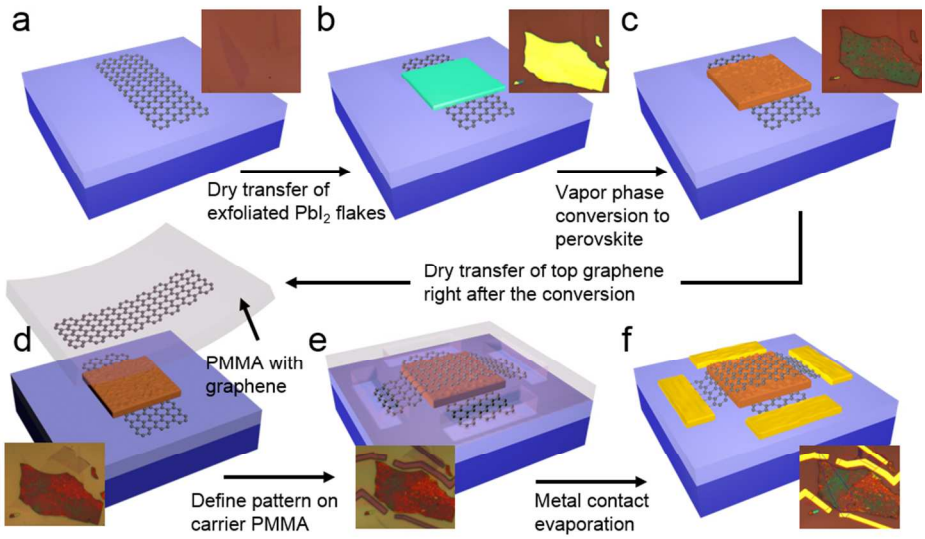

Figure S4. Schematics and optical images for each of steps of GPG device fabrication process. (a) The bottom-graphene was first exfoliated on the top of 290 nm SiO_2/highly doped Si substrate. (b) The PbI_2 was exfoliated into small flakes and transferred to graphene. (c) The PbI_2/graphene stack was then converted into perovskite in the furnace with methylammonium iodide vapor carried by argon gas flow. (d) The as-converted perovskite was immediately covered with the separately prepared graphene/carrier PMMA stack. (e) The electrode patterns were defined directly on the carrier PMMA by e-beam lithography without additional spin-coating process. (f) After metal evaporation, the device was lift-off in chloroform.

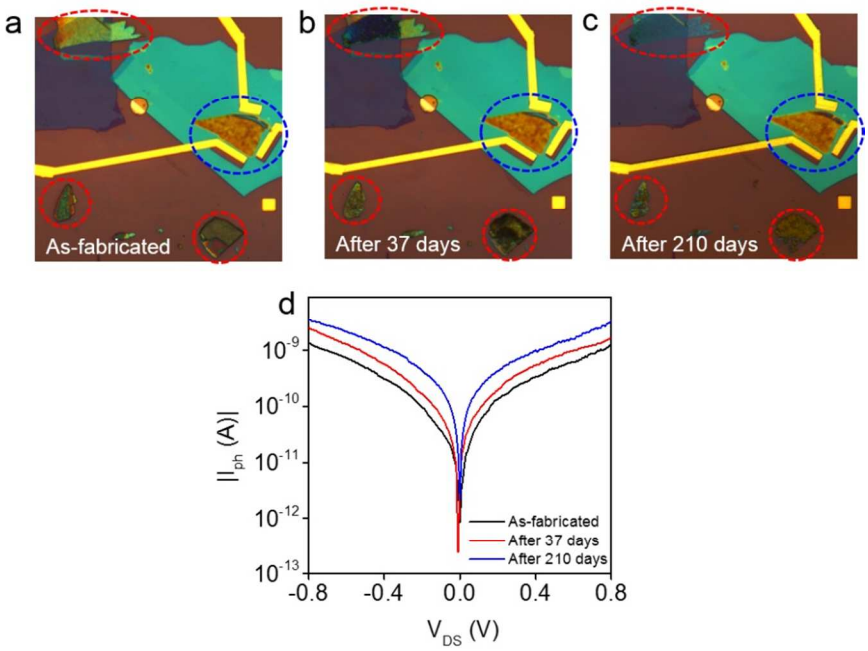

Figure S5. Improved stability of BN-covered GPG device. (a) Optical image of a BN-covered GPG device taken right after lift-off process. The red dashed circles indicate some other perovskite flakes that were not covered by BN, while the BN-covered device is indicated by a blue dashed circle. (b) Optical image of the same spot taken after 37 days stored in desiccator. All exposed perovskite flakes showed some damage, especially the one sitting on the multilayer graphene (upper left corner) had a considerable damage compared other part that sitting on the SiO_2. It might be due to the reactivity of graphene that accelerates the decomposition of perovskite. On the other hand, no visible damage was observed in BN-covered device. (c) Optical image of the same spot taken after 210 days stored in desiccator. The uncovered flakes were seriously damaged, while the covered device remains intact. (d) The logarithmic plots of photocurrent $I_{ph} = (I_{illuminated} - I_{dark})$ versus bias voltage were obtained by measuring at the conditions shown in (a), (b) and (c). No degradation in terms of photocurrent performance was observed. The photocurrent gain seems to increase over time, the reason for that is unclear, possibly due to the improved contact between perovskite and graphene.

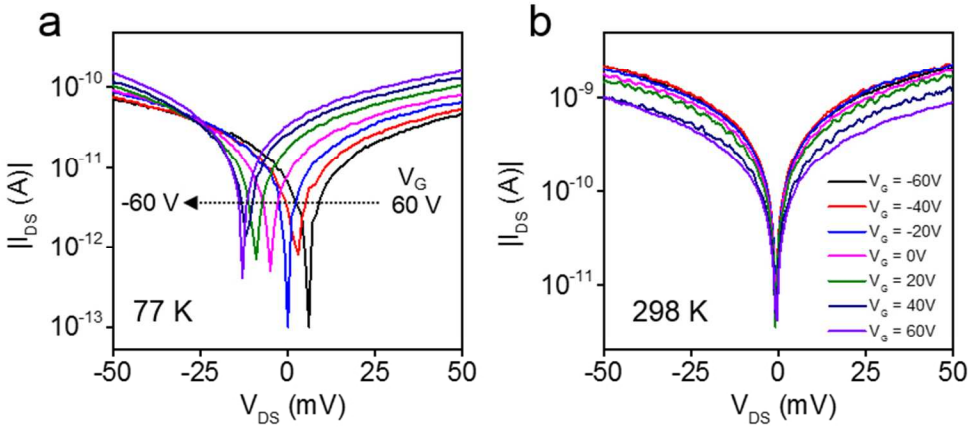

Figure S6. Gate-tunable photovoltaic effect in GPG device. (a) The illuminated I_{DS}-V_{DS} curves of GPG device measured at 77 K with the back gate voltage swept from 60V to -60V, which shows a consistent V_{OC} shift as the one shown in Fig. 3d of the main text (from -60 V to 60 V). (b) Room temperature measurement of the same device shown in (a). No gate-dependent V_{OC} shift was obtained.

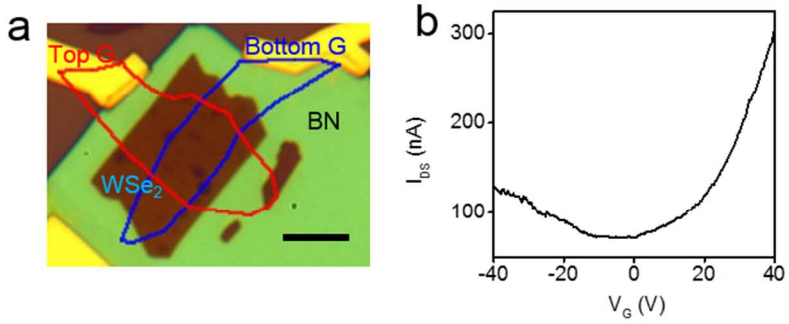

Figure S7. Ambipolarity of graphene/WSe_2/graphene (GWG) heterostructure device. (a) Optical image of GWG device. The red and blue lines framed the top- and bottom-graphene. A WSe_2 flake with similar thickness to GWPG device was used. The black scale bar is 5 μm. (b) An ambipolar transfer characterisitic of GWG device was obtained with bias voltage = -0.5 V.

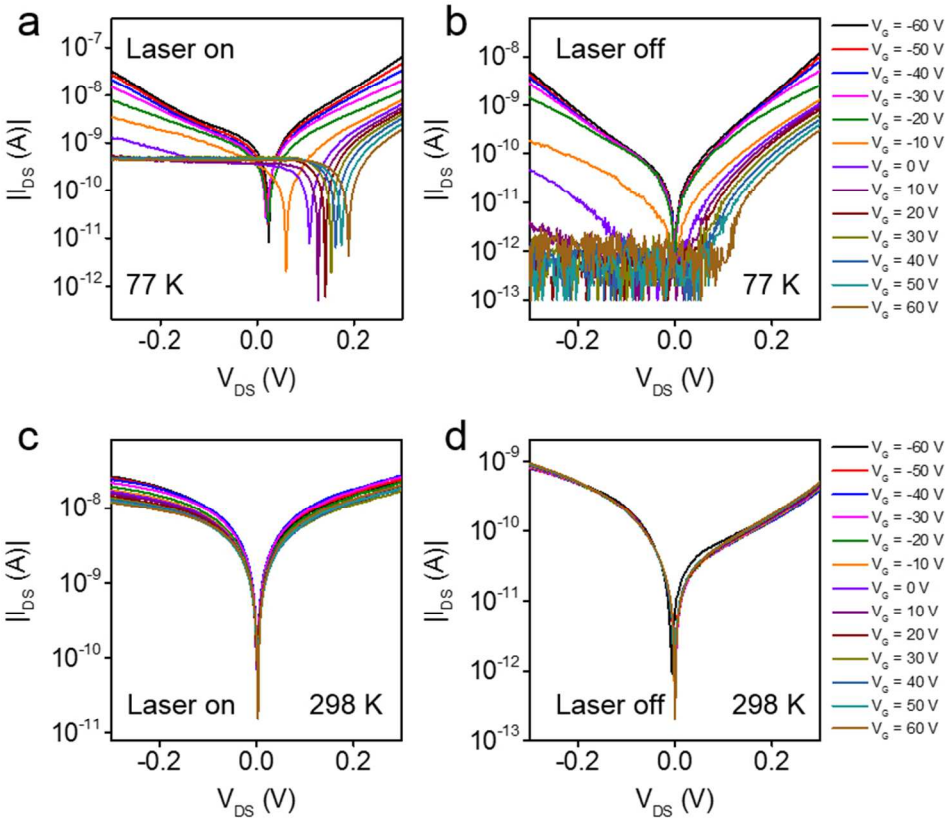

Figure S8. Gate-tunable photovoltaic effect in GWPG device. (a, b) Logarithmic plot of I_{DS}-V_{DS} characteristics of GWPG device measured at 77 K with/without 532 nm laser illumination, respectively. Under illumination, the V_{OC} can be effectively modulated by gate voltage. The dark I_{DS}-V_{DS} shows a distinct transition from p-p to n-p regime. (c, d) Room temperature measurement of the same device shown in (a, b). No p-p to n-p transition and gate-tuning V_{OC} were observed.

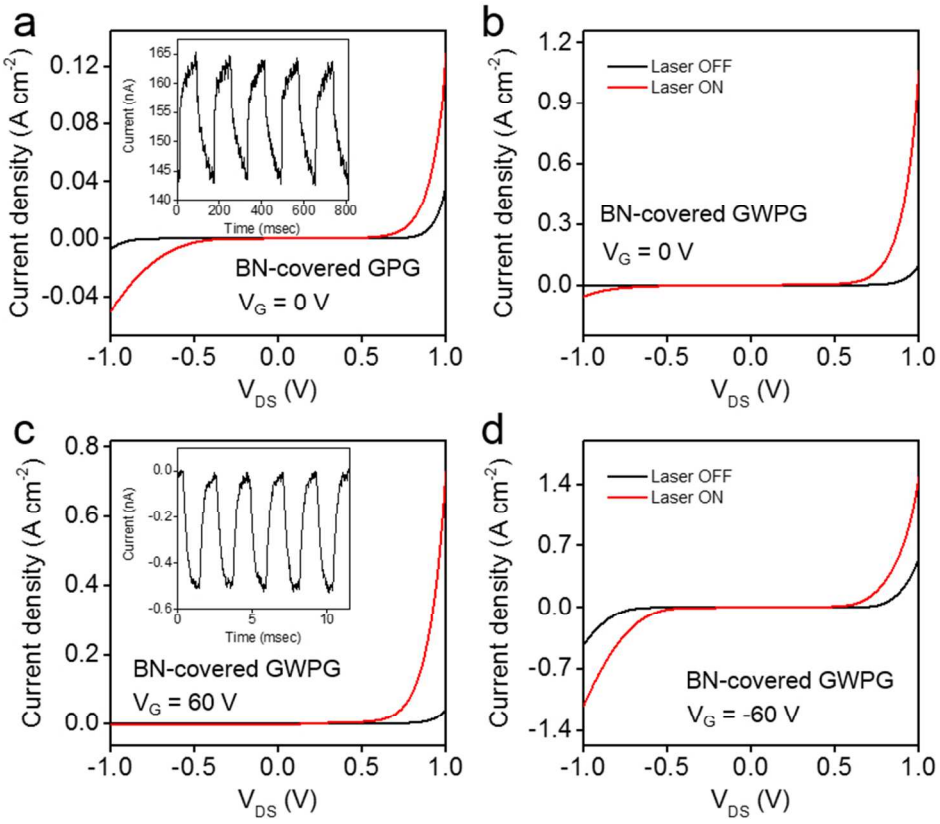

Figure S9. Photoresponse of BN-covered GPG and GWPG device (a) The BN-covered GPG device has a photoconductive gain of 143 (61.6 A/W) at V_{DS} = 1 V, V_G = 0 V. The inset shows the time-domain response at 1V (with rise time ~30 ms and fall time ~48 ms). (b) The photoconductive gain for BN-covered GWPG at V_{DS} = 1 V, V_G = 0 V is ~1495 (642 A/W) (c) At V_G = 60 V, the GWPG device is tuned to be a p-n diode. A diode rectifying behavior was observed, which has a photoconductive gain ~1072 (456 A/W) at V_{DS} = 1V. The inset shows the time-domain photoresponse at zero bias with a rise time ~436 μs and fall time 540 μs. (c) At V_G = -60 V, the device become symmetric p-p junction device (with a gain ~1437 (616.5 A/W) at V_{DS} = 1 V). All measurements were conducted at 77 K.

Reference

1. Sandroff, C. J.; Kelty, S. P.; Hwang, D. M. *J. Chem. Phys* **1986,** 85, (9), 5337-5340.

2. Goto, T.; Maeda, J. *J. Phys. Soc. Jpn.* **1987,** 56, (10), 3710-3714.